Supplementary Information for

Thermal Transport at the Nanoscale: A Fourier's Law vs. Phonon Boltzmann Equation Study

Jan Kaiser[1], Tianli Feng[3], Jesse Maassen[2], Xufeng Wang[3], Xiulin Ruan[3], and Mark Lundstrom[3]

[1]Ruhr-University Bochum, [2]Dalhousie University, [3]Purdue University

December 22, 2016

1. Obtaining the McKelvey-Shockley equations from the EPRT

Deriving the flux equations from the full BTE requires a careful discussion of the relaxation time approximation, the time-derivative term, conservation of energy, and other issues. Here, we simply indicate how the flux equations relate to the steady-state equation of phonon radiative transfer (EPRT) [7],

$$\mu \frac{dI_\omega}{dx} = \frac{I_\omega^0 - I_\omega}{\upsilon\tau}, \tag{S1a}$$

which is often the starting point for thermal analysis. In (S1a), $I_\omega(\theta,\phi)$ is the phonon intensity in the direction (θ,ϕ), $\mu = \cos\theta$ is the cosine of the angle between the phonon propagation direction and the x-axis, $\upsilon(\theta,\phi)$ is the phonon velocity in the direction (θ,ϕ), $\tau(\omega)$ is an energy-dependent scattering time, and I_ω^0 is the equilibrium phonon intensity. Equation (S1a) can be re-written as

$$\upsilon\tau\mu \frac{dI_\omega}{dx} = I_\omega^0 - I_\omega. \tag{S1b}$$

Now recognize that I_ω^0 is symmetric in the x-direction, but $I_\omega^0 - I_\omega$ is anti-symmetric, because there is a net heat current in the x-direction. The phonon intensity can be decomposed into symmetric and anti-symmetric components. If we assume near equilibrium conditions, the symmetric component is I_ω^0, therefore, $I_\omega^0 - I_\omega$ is the anti-symmetric component, which can be written as

$$I_\omega^0 - I_\omega = \frac{I_\omega(\mu>0) - I_\omega(\mu<0)}{2}. \tag{S2}$$

Using (S2) in (S1b), we find

$$\frac{d}{dx}(2\upsilon\tau\mu I_\omega) = -I_\omega(\mu>0) + I_\omega(\mu<0), \tag{S3}$$

and by integrating (S3) over the forward directions, $\mu>0$, we find

$$\frac{d}{dx}\int(2\upsilon\tau\mu I_\omega)\,d\Omega^+ = -\int I_\omega(\mu>0)\,d\Omega^+ + \int I_\omega(\mu<0)\,d\Omega^+ . \tag{S4}$$

Integrating the intensity distribution over angles is like the well-known "differential approximation" [22], but here, we separately integrate over the forward and reverse directions. We can recognize the forward flux in the McKelvey-Shockley equations as

$$F_Q^+ = \int I_\omega(\mu>0)\,d\Omega^+ . \tag{S5a}$$

Similarly, the negative flux is the magnitude of the heat flowing in the –x-direction,

$$F_Q^- = \int I_\omega(\mu<0)\,d\Omega^- . \tag{S5b}$$

Using these definitions, (S4) becomes

$$\frac{d}{dx}\int(2\upsilon\tau\mu I_\omega)\,d\Omega^+ = -F_Q^+ + F_Q^- . \tag{S6}$$

Next, we divide and multiply on the LHS by the forward flux to write

$$\frac{d}{dx}\left[\frac{\int(2\upsilon\tau\mu I_\omega)\,d\Omega^+}{\int I_\omega\,d\Omega^+}\int I_\omega\,d\Omega^+\right] = -F_Q^+ + F_Q^- . \tag{S7}$$

The next step is to define the "mean-free-path for backscattering,"

$$\lambda \equiv \frac{\int \left(2\upsilon\tau\mu I_\omega\right) d\Omega^+}{\int I_\omega \, d\Omega^+} = \frac{\int \left(2\Lambda\mu I_\omega\right) d\Omega^+}{\int I_\omega \, d\Omega^+}, \tag{S8}$$

where $\Lambda = \upsilon\tau$ is the conventional mean-free-path. Using (S8), we write (S7) as

$$\frac{d}{dx}\left[\lambda F_Q^+\right] = -F_Q^+ + F_Q^- . \tag{S9}$$

Finally, we argue that although I_ω^+ varies with position, only its magnitude changes; its shape does not change as long as we are near equilibrium. Accordingly, λ is spatially uniform, so it may be moved out of the derivative in (S9) to write

$$\frac{dF_Q^+}{dx} = -\frac{F_Q^+}{\lambda} + \frac{F_Q^-}{\lambda}, \tag{S10}$$

which is the McKelvey-Shockley equation for the forward flux, eqn. (1a). A similar argument gives eqn. (1b) for the negative flux.

The reader may be concerned about the near-equilibrium assumption used to arrive at eqn. (S2). This assumption does not hold in the ballistic limit, but in this case, the scattering time (mean-free-path) approaches infinity, and the scattering term, where this approximation is used, approaches zero. Accordingly, the near-equilibrium assumption should introduce no error in the diffusive limit, where it is valid nor in the ballistic limit, where it is irrelevant. This assumption may be the source of error we observe between the diffusive and ballistic limits.

2. Derivation of the heat equations

With a uniform heat generation term, $\dot{S}$, the steady-state flux equations are:

$$\frac{dF_Q^+(x)}{dx} = -\frac{F_Q^+(x)}{\lambda} + \frac{F_Q^-(x)}{\lambda} + \frac{\dot{S}}{2} \tag{S11a}$$

$$\frac{dF_Q^-(x)}{dx} = -\frac{F_Q^+(x)}{\lambda} + \frac{F_Q^-(x)}{\lambda} - \frac{\dot{S}}{2}. \tag{S11b}$$

The net heat flux is

$$F_Q\left(x\right) = F_Q^+(x) - F_Q^-(x). \tag{S12}$$

Subtract (S11b) from (S11a) to find

$$\frac{dF_Q}{dx} = \dot{S}. \tag{S13}$$

Add (S11a) and (S11b) to find

$$\frac{d\left(F_Q^+ + F_Q^-\right)}{dx} = -\frac{2F_Q}{\lambda}$$

$$F_Q = -\frac{\lambda}{2}\frac{d\left(F_Q^+ + F_Q^-\right)}{dx}. \tag{S14}$$

Assuming the validity of the simplified BTE we began with, eqn. (S11), these equations are exact. Now we must define temperature.

3. Definition of temperature at the nanoscale

Let's begin with the equilibrium fluxes:

$$F_{Q0}^{+/-} = \frac{C_V\left(T_0\right)}{2}\upsilon_x^+ T_0. \tag{S15}$$

For a small temperature deviations from the equilibrium reference:

$$F_Q^{+/-}\left(x\right) = \frac{C_V\left(T_0\right)}{2}\upsilon_x^+\left(T_0 + \delta T^{+/-}\left(x\right)\right) = \frac{C_V\left(T_0\right)}{2}\upsilon_x^+ T^{+/-}\left(x\right), \tag{S16}$$

where

$$T^{+/-}\left(x\right) = T_0 + \delta T^{+/-}\left(x\right). \tag{S17}$$

Using (S14) and noting that

$$\frac{dT^{+/-}}{dx} = \frac{d\left(\delta T^{+/-}\right)}{dx},$$

we find

$$F_Q = -\frac{\lambda\upsilon_x^+ C_V\left(T_0\right)}{2}\frac{d\left(T^+ + T^-\right)/2}{dx}, \tag{S18}$$

where we are assuming that the mean-free-path and specific heat are independent of position. Finally, we obtain:

$$F_Q = -\kappa_{bulk}\frac{dT}{dx} \tag{S19a}$$

$$\kappa_{bulk} = \frac{\upsilon_x^+\lambda}{2}C_v\left(T_0\right) \tag{S19b}$$

$$T = \left(T^+ + T^-\right)/2. \tag{S19c}$$

4. Boundary conditions

Proper boundary conditions for the BTE are the incident fluxes from the two contacts. We must use these same b.c.'s in the equivalent diffusion equations. Consider the left contact shown in Fig. S1.

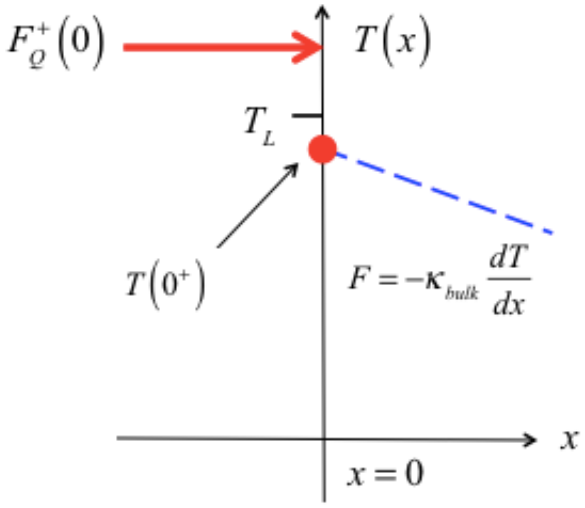

Fig. S1. Boundary conditions at the left contact.

At x = 0^+, the net flux is

$$F_Q(0^+)=F_Q^+(0^+)-F_Q^-(0^+), \tag{S20a}$$

which is also

$$F_Q(0^+)=-\kappa_{bulk}\left.\frac{dT}{dx}\right|_{x=0^+}. \tag{S20b}$$

The incident fluxes (the proper boundary conditions for the BTE) are

$$F_Q^+(x=0^+)=v_x^+\frac{C_v}{2}T^+(x=0^+)=v_x^+\frac{C_v}{2}T_L \tag{S21a}$$

$$F_Q^-(x=L^-)=v_x^+\frac{C_v}{2}T^-(x=L^-)=v_x^+\frac{C_v}{2}T_R. \tag{S21b}$$

In these equations, the parameters, specific heat and average +x-directed velocity, describe the film; the temperature is that of the metal. (We are assuming that C_v is evaluated at the reference temperature, T_0.)

At $x=0^+$, we add the forward and reverse fluxes in the film to find

$$F_Q^+\left(0^+\right)+F_Q^-\left(0^+\right)=T^+\left(0^+\right)\frac{C_v}{2}\upsilon_x^+ + T^-\left(0^+\right)\frac{C_v}{2}\upsilon_x^+$$

or

$$F_Q^+\left(0^+\right)+F_Q^-\left(0^+\right)=C_v\upsilon_x^+\left(\frac{T^+\left(0^+\right)+T^-\left(0^+\right)}{2}\right).$$

By using

$$T\left(0^+\right)=\left(\frac{T^+\left(0^+\right)+T^-\left(0^+\right)}{2}\right),$$

we find

$$F_Q^+\left(0^+\right)+F_Q^-\left(0^+\right)=C_v\upsilon_x^+\frac{T\left(0\right)}{2}. \tag{S22}$$

From (S20a) and (S20b) we have

$$-\kappa_{bulk}\left.\frac{dT}{dx}\right|_{x=0^+}=F_Q^+\left(0^+\right)-F_Q^-\left(0^+\right),$$

and from (S12)

$$F_Q^-\left(0^+\right)=C_v\upsilon_x^+\frac{T\left(0\right)}{2}-F_Q^+\left(0^+\right).$$

From the above two equations, we find

$$-\kappa_{bulk}\left.\frac{dT}{dx}\right|_{x=0^+}+C_vT\left(0^+\right)\upsilon_x^+=2F_Q^+\left(0\right), \tag{S23}$$

which is the boundary condition at x = 0. Similar arguments can be made for the boundary condition at x = L.

In summary, the boundary conditions at x = 0 and x =L are

$$-\kappa_{bulk}\left.\frac{dT}{dx}\right|_{x=0^+}+C_vT\left(0^+\right)\upsilon_x^+=2F_Q^+\left(0\right) \tag{S24a}$$

$$-\kappa_{bulk}\left.\frac{dT}{dx}\right|_{x=L^-}-C_vT\left(L^-\right)\upsilon_x^+=-2F_Q^-\left(L\right). \tag{S24b}$$

Note that $F_Q^+\left(0\right)$ is incident flux at x = 0, which is known because it is the flux injected from the equilibrium metal contact at the left. Also, $F_Q^-\left(L\right)$ is known. We cannot specify the temperatures at the two ends – <u>we can only specify the incident heat fluxes.</u>

Alternative view of boundary conditions: ballistic resistors at x = 0 and x = L.

From (S24a), we have

$$F_Q(0) = -\kappa_{bulk}\left.\frac{dT}{dx}\right|_{x=0^+} = 2F_Q^+(0) - C_v T(0^+)\upsilon_x^+ .$$

Using (S11a) for $F_Q^+(x=0^+) = F_Q^+(0)$, this becomes

$$F_Q(0) = 2\left[\frac{C_v}{2}\upsilon_x^+ T^+(0^+)\right] - C_v\upsilon_x^+ T(0^+),$$

or

$$F_Q(0) = C_v\upsilon_x^+\left[T^+(0^+) - T(0^+)\right]. \tag{S25}$$

In terms of heat current $I_Q(0) = AF_Q(0)$ (not heat current density), (S25) becomes

$$I_Q(0) = AC_v\upsilon_x^+\left[T^+(0^+) - T(0^+)\right] \tag{S26}$$

Note that

$$T^+(0^+) = T_L,$$

In words, the forward temperature at x = 0 is the temperature of the left contact, which is known. Finally, we write the temperature jump as

$$\Delta T(0) = I_Q(0)\frac{R_B}{2}, \tag{S27a}$$

where

$$\Delta T(0) = \left[T_L - T(0^+)\right] \tag{S27b}$$

$$R_B = \frac{2}{AC_v\upsilon_x^+} \tag{S27c}$$

is the ballistic thermal resistance.

In summary, the boundary conditions in terms of the ballistic thermal resistance are:

$$\Delta T(0) = F_Q(0)\frac{R_B A}{2} \tag{S28a}$$

$$\Delta T(L) = F_Q(L)\frac{R_B A}{2}, \tag{S28b}$$

where the ballistic thermal resistance is

$$R_B A = \frac{2}{C_v \upsilon_x^+}\,, \tag{S29}$$

and the temperature jumps are defined as

$$\Delta T(0) = \left[T_L - T\left(0^+\right) \right] \tag{S30a}$$

$$\Delta T(L) = \left[T\left(L^-\right) - T_R \right]. \tag{S30b}$$

5. Directed temperatures

After solving Fourier's Law and the heat equation for T(x), can we deduce the directed temperatures, $T^+(x)$ and $T^-(x)$ from our solutions?

From Fourier's Law:

$$F_Q = -\kappa_{bulk} \frac{dT}{dx},$$

we can write:

$$F_Q = -\frac{\kappa_{bulk}}{2} \frac{d\left(T^+ + T^-\right)}{dx},$$

and solve for

$$\frac{dT^+(x)}{dx} + \frac{dT^-(x)}{dx} = -\frac{2F_Q}{\kappa_{bulk}}. \tag{S31a}$$

The net heat flux can also be written as

$$F_Q = \frac{C_V}{2} \upsilon_x^+ \left(T^+(x) - T^-(x) \right),$$

which can be differentiated to find (use (S13))

$$\frac{dT^+(x)}{dx} - \frac{dT^-(x)}{dx} = \frac{2\dot{S}}{C_V \upsilon_x^+}. \tag{S31b}$$

(S31a) and (S31b) are two equations in two unknowns. We can solve these two equations to find

$$\frac{dT^+(x)}{dx} = \frac{dT(x)}{dx} + \frac{\dot{S}}{C_v \upsilon_x^+} \tag{S32a}$$

$$\frac{dT^-(x)}{dx} = \frac{dT(x)}{dx} - \frac{\dot{S}}{C_v \upsilon_x^+}. \tag{S32b}$$

In these equations, $T(x)$ is known from the solution and $T^+(x=0)=T_L$ and $T^-(x=L)=T_R$. Equations (S32a) and (S32b) can be integrated to find

$$T^+(x)-T_L=T(x)-T(0)+\frac{\dot{S}}{C_v\upsilon_x^+}x \tag{S33a}$$

$$T^-(x)-T_R=T(x)-T(L)+\frac{\dot{S}}{C_v\upsilon_x^+}(L-x). \tag{S33b}$$

These equations are correct, but they can be written more simply in terms of the ballistic thermal resistance.

Begin with (S33a) and write it as

$$T^+(x)=T(x)+T_L-T(0)+\frac{\dot{S}}{C_v\upsilon_x^+}x,$$

or

$$T^+(x)=T(x)+\Delta T(0)+\frac{\dot{S}}{C_v\upsilon_x^+}x,$$

which, using (S28a), is

$$T^+(x)=T(x)+I_Q\frac{R_B}{2}+\frac{\dot{S}}{C_v\upsilon_x^+}x\ . \tag{S34}$$

Now solve

$$\frac{dF_Q}{dx}=\dot{S}$$

for

$$F_Q(x)=F_Q(0)+\dot{S}x.$$

Use this result in (S34) to find

$$T^+(x)=T(x)+I_Q(0)\frac{R_B}{2}+\frac{F_Q(x)-F_Q(0)}{C_v\upsilon_x^+}$$

$$T^+(x)=T(x)+I_Q(0)\frac{R_B}{2}+\frac{I_Q(x)-I_Q(0)}{AC_v\upsilon_x^+}$$

$$T^+(x)=T(x)+I_Q(0)\frac{R_B}{2}+I_Q(x)\frac{R_B}{2}-I_Q(0)\frac{R_B}{2},$$

which leads to the final result

$$T^{+}(x) = T(x) + I_Q(x)\frac{R_B}{2} \tag{S35a}$$

$$T^{-}(x) = T(x) - I_Q(x)\frac{R_B}{2}. \tag{S35b}$$

The directed temperatures provide a clear way to think about temperature at the nanoscale. How does this approach compare to other definitions? According to eqns. (S16)

$$F_Q^{+}(x) = \frac{C_V(T_0)}{2}\upsilon_x^{+}T^{+}(x)$$

$$F_Q^{-}(x) = \frac{C_V(T_0)}{2}\upsilon_x^{+}T^{+}(x)$$

from which we find

$$T^{+}(x) = \frac{2F_Q^{+}(x)}{C_V(T_0)\upsilon_x^{+}} \tag{S36a}$$

$$T^{-}(x) = \frac{2F_Q^{-}(x)}{C_V(T_0)\upsilon_x^{+}}. \tag{S36b}$$

Using (S19c), we find

$$T(x) = \frac{T^{+}(x) + T^{-}(x)}{2} = \frac{F_Q^{+}(x) + F_Q^{-}(x)}{C_V(T_0)\upsilon_x^{+}} = \frac{F_Q^{tot}(x)}{C_V(T_0)\upsilon_x^{+}}, \tag{S37}$$

where $F_Q^{+}(x) + F_Q^{-}(x)$ is the sum of the forward and backward directed fluxes. Next, we write $F_Q^{tot}(x)$ as

$$F_Q^{tot}(x) = 4\pi e(x)\upsilon_x^{+}, \tag{S38}$$

where $e(x)$ is the energy density per steradian. Using (S38) in S37), we find

$$T(x) = \frac{4\pi e(x)}{C_V(T_0)}, \tag{S39}$$

which is a commonly used definition of temperature. Our definition in terms of temperatures associated with the forward and backward fluxes provides a physical justification for (S39) out of equilibrium.

6. The ballistic solution

Begin with the flux equations, (S10a) and (S10b) in the ballistic limit, $\lambda \to \infty$ to find

$$\frac{dF_Q^+(x)}{dx} = +\frac{\dot{S}}{2} \tag{S40a}$$

$$\frac{dF_Q^-(x)}{dx} = -\frac{\dot{S}}{2}\,. \tag{S40b}$$

Recall how the forward and backward fluxes are related to the forward and backward stream temperatures:

$$F_Q^+ = \upsilon_x^+ \frac{C_v}{2} T^+$$
$$F_Q^- = \upsilon_x^+ \frac{C_v}{2} T^-,$$

which can be used in (S40) to find

$$\frac{dT^+(x)}{dx} = +\frac{\dot{S}}{\upsilon_x^+ C_v}$$
$$\frac{dT^-(x)}{dx} = -\frac{\dot{S}}{\upsilon_x^+ C_v}.$$

After integrating these equations, we find

$$T^+(x) = T_L + \left(\frac{\dot{S}}{\upsilon_x^+ C_v}\right) x \tag{S41a}$$

$$T^-(x) = T_R + \left(\frac{\dot{S}}{\upsilon_x^+ C_v}\right)\left(L - x\right). \tag{S41b}$$

From the definition of temperature, we find:

$$T\left(x\right) = \frac{T^+(x) + T^-(x)}{2} = \frac{T_L + T_R}{2} + \left(\frac{\dot{S}L}{2\upsilon_x^+ C_v}\right).$$

The final result is

$$T\left(x\right) = \frac{T_L + T_R}{2} + \left(\frac{\dot{S}L}{2\upsilon_x^+ C_v}\right). \tag{S42}$$

Case 1: Cross-plane with a temperature difference but no heat source.

According the (S42), the ballistic solution is:

$$T(x) = \frac{T_L + T_R}{2} \quad . \tag{S43a}$$

The Fourier's Law solution is given by eqns. (16) and (17) in the text. In the ballistic limit, $\kappa_{bulk} \to \infty$, this solution gives the same result for the ballistic limit, (S43a).

Case 2: Cross-plane with no temperature difference but with an internal heat source

According the (S42), the ballistic solution is:

$$T(x) = T_0 + \left(\frac{\dot{S}L}{2\upsilon_x^+ C_v} \right), \tag{S43b}$$

where $T_0 = T_L = T_R$. The Fourier's Law solution is given by eqns. (18) and (19) in the text. In the ballistic limit, $\kappa_{bulk} \to \infty$, this solution gives the same result for the ballistic limit, (S43b).

7. Summary of equations

We solve the conventional heat equation:

$$\frac{d^2T}{dx^2} = -\frac{\dot{S}}{\kappa_{bulk}} \tag{S44a}$$

with the unconventional boundary conditions:

$$\Delta T(0) = T_L - T(0^+) = F_Q(0)\frac{R_B A}{2} \tag{S44b}$$

$$\Delta T(L) = T(L^-) - T_R = F_Q(L)\frac{R_B A}{2} . \tag{S44c}$$

where the ballistic thermal resistance is given by

$$R_B A = \frac{2}{C_v \upsilon_x^+} . \tag{S44d}$$

After solving for $T(x)$, the directed temperatures can be obtained from

$$T^+(x) = T(x) + I_Q(x)\frac{R_B}{2} \tag{S44e}$$

$$T^-(x) = T(x) - I_Q(x)\frac{R_B}{2} . \tag{S44f}$$

8. Solution: Temperature difference with no internal heat generation

The figure below shows the problem to be solved.

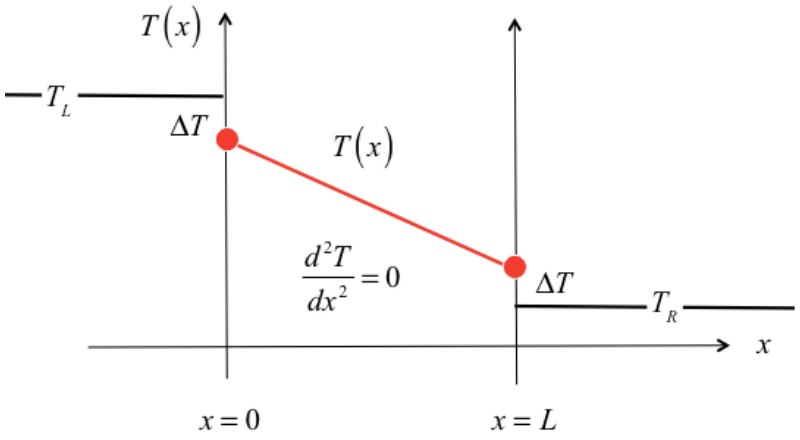

Fig. S2 Temperature vs. position for the case of contacts with different temperatures and no internal heat generation.

The heat flux is:

$$F_Q = \kappa_{bulk}\left(\frac{T_L - \Delta T - \left(T_R + \Delta T\right)}{L}\right)$$

with the boundary condition:

$$\Delta T = F_Q \frac{R_B A}{2}.$$

These two equations give

$$F_Q = \kappa_{bulk}\left(\frac{T_L - T_R - 2\Delta T}{L_x}\right) = \kappa_{bulk}\left(\frac{T_L - T_R - \left(R_B A\right)F_Q}{L_x}\right)$$

$$F_Q\left(1 + \frac{\kappa_{bulk} R_B A}{L_x}\right) = \kappa_{bulk}\left(\frac{T_L - T_R}{L_x}\right). \qquad \text{(S45)}$$

From (S9b) and (S17c),

$$\kappa_{bulk} R_B A = \frac{\upsilon_x^+ \lambda}{2}\frac{2}{\upsilon_x^+ C_V} = \lambda,$$

so (S31) becomes

$$F_Q\left(1+\frac{\lambda}{L_x}\right)=\kappa_{bulk}\left(\frac{T_L-T_R}{L_x}\right)$$

$$F_Q=\frac{\kappa_{bulk}}{\left(1+\lambda/L_x\right)}\left(\frac{T_L-T_R}{L_x}\right)=\kappa_{app}\left(\frac{T_L-T_R}{L_x}\right). \tag{S46}$$

and we have derived eqns. (14) and (15) of the text.

9. Solution: No temperature difference with internal heat generation

In this case, we solve

$$\frac{d^2T}{dx^2}=-\frac{\dot{S}}{\kappa_{bulk}}\ .$$

The general solution is

$$T\left(x\right)=-\left(\frac{\dot{S}}{\kappa_{bulk}}\right)\frac{x^2}{2}+c_1x+c_2\ . \tag{S47}$$

Assume that the left and right contacts are at temperature, T_0. At the two ends of the film,

$$T\left(0^+\right)=T\left(L_x^-\right)=T_b\neq T_0\ .$$

The temperatures at the boundaries of the film, $T\left(0^+\right)=T\left(L_x^-\right)$, cannot be imposed, they are a result of the calculation. Since the two boundary temperatures are identical, the general solution, (S47), gives in this case

$$T\left(x\right)=\left(\frac{\dot{S}}{2\kappa_{bulk}}\right)\left(L-x\right)x+T_b, \tag{S48}$$

and we must determine the boundary temperature, T_b. The situation is shown in the figure below.

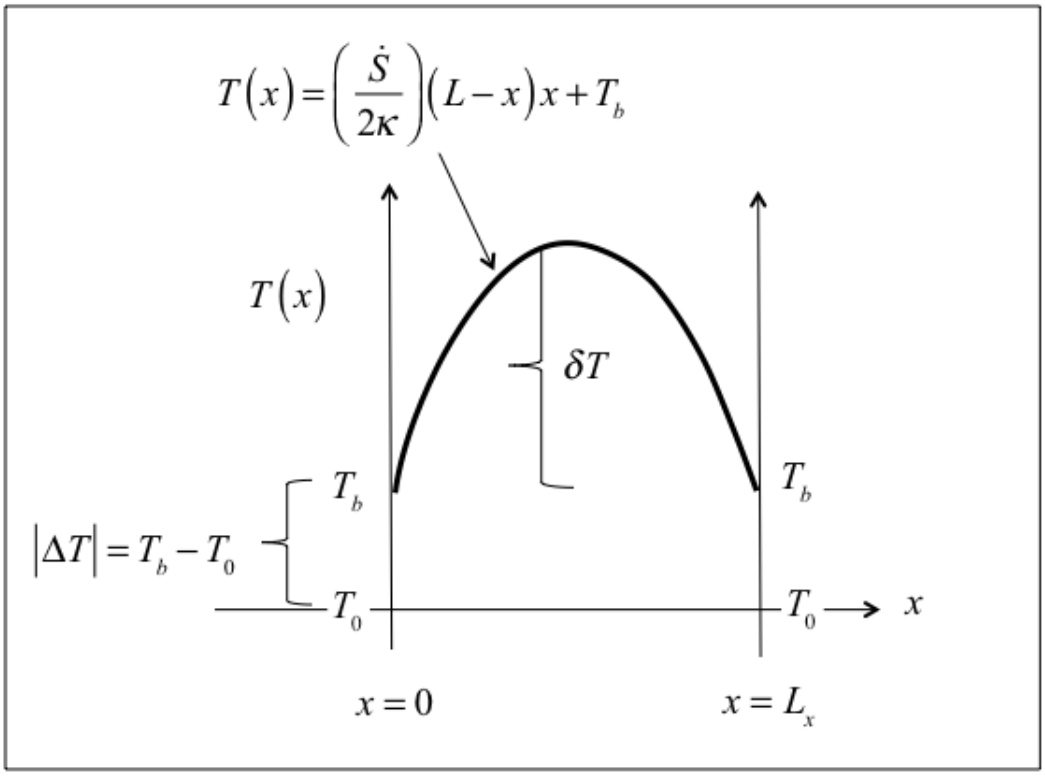

Fig. S3 Temperature vs. position for the case of contacts with the same temperatures and with uniform internal heat generation.

The temperature at the x = 0 boundary is given by:

$$T_b - T_0 = -F_Q(0)\frac{R_B A}{2}. \tag{S49}$$

The temperature jump is **up** as we go from the metal to the film, rather than **down**, as we assumed when defining ΔT in eqn. (9a) of the text, so we have a minus sign in the equation above.

The heat flux at x = 0 is

$$F_Q(0) = -\kappa_{bulk}\left.\frac{dT}{dx}\right|_{x=0^+}.$$

Using (S44), we find

$$\frac{dT(x)}{dx} = \left(\frac{\dot{S}}{2\kappa_{bulk}}\right)(L-2x),$$

which gives

$$\left.\frac{dT(x)}{dx}\right|_{x=0^+} = \left(\frac{\dot{S}L}{2\kappa_{bulk}}\right)$$

at x = 0. This gives a heat flux at x = 0 that is

$$F_Q(0) = -\kappa_{bulk}\left(\frac{\dot{S}L}{2\kappa_{bulk}}\right) = \frac{\dot{S}L}{2}, \tag{S50}$$

which is intuitively obvious.

Equation (S50) can be used in (S49) to find

$$T_b - T_0 = \left(\frac{\dot{S}L}{2}\right)\frac{R_B A}{2}. \tag{S51}$$

Using the definition of ballistic thermal resistance,

$$R_B A = \frac{2}{C_v \upsilon_x^+},$$

eqn. (S51) becomes

$$\Delta T = T_b - T_0 = \left(\frac{\dot{S}L}{2}\right)\frac{1}{C_v \upsilon_x^+}. \tag{S52}$$

which is independent of the mean-free-path.

To summarize, the solution is:

$$T(x) = \left(\frac{\dot{S}}{2\kappa_{bulk}}\right)(L-x)x + T_b \tag{S53a}$$

$$T_b = T_0 + \left(\frac{\dot{S}L}{2}\right)\frac{1}{C_v \upsilon_x^+}. \tag{S53b}$$

It is interesting to note that even for $L_x >> \lambda$ (diffusive limit), there is a temperature jump at the contacts. This is an example of where the conventional application of Fourier's Law (which assumes $T(0) = T(L_x) = T_0$) fails – even for films many mean-free-paths long. In practice, however, we expect that $\Delta T << \delta T$, so the effect would be hard to observe.

Suggested exercises:

1) Repeat the derivation but do not assume that the two contacts are at the same temperature.

2) Repeat the derivation for a delta-function heat source at the center of the film.

10. Comparisons to Monte Carlo simulations of Hua and Cao

In this section, we present comparisons of Fourier's Law solutions to the Monte Carlo simulation results of Hua and Cao [16, 18].

Temperature difference but no internal heat generation

Consider first the case of a temperature difference (TD) between the two contacts, but no internal heat generation (IHG). The normalized temperature profiles for three different Knudsen numbers are plotted in Fig. S4, which compares the Fourier's Law solution as given by eqn. (16) to Monte Carlo simulations from [16]. In the diffusive limit, $T(x)$ varies linearly from T_L to T_R and both solutions agree. In the ballistic limit (not shown in Fig. S4), $T(x)=(T_L+T_R)/2$, and Fourier's Law gives the correct answer. Figure S4 shows a small difference in the quasi-ballistic regime ($Kn_x \approx 5.0$), which would presumably get smaller if the Knudsen number were larger. For this case (which is much like the case treated in [9]), Fourier's Law provides a good description of ballistic to diffusive transport. Figure S4 should be compared to Fig. 3a of the text.

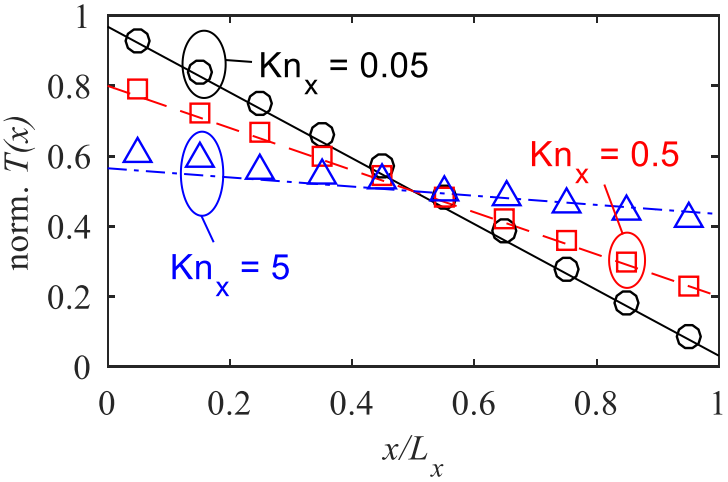

Fig. S4. Normalized temperature profile $(T(x)-T_R)/(T_L-T_R)$ vs. normalized distance, x/L_x, for cross-plane heat transport with no internal heat generation (case a) in Fig. 1). Three different Knudsen numbers are shown. Lines are the result of Fourier's Law, and circles are Monte Carlo simulations taken from [18].

Figure S5, a plot of $\Delta T(0)/(T_L-T_R)$ vs. Kn_x for case 1a (cross-plane thermal transport without internal heat generation) compares Fourier's Law and Monte Carlo solutions. Fourier's Law predicts a temperature jump that rises from zero to $0.5(T_L-T_R)$ as Kn_x increases from $Kn_x << 1$ to $Kn_x >> 1$. A temperature jump of $0.5(T_L-T_R)$ is expected in the ballistic limit [12, 24]. Figure S5 shows good agreement between Fourier's Law and Monte

Carlo solutions for small Kn_x, but for large Kn_x, the Monte Carlo results are about 5% below the Fourier's Law solution. Good agreement is expected for very large Kn_x (the ballistic limit). It is possible that the Monte Carlo simulations would approach the correct ballistic limit at very large Knudson number, but it may also be that small numerical errors are preventing the Monte Carlo simulations from reaching the correct ballistic limit of $0.5\left(T_L - T_R\right)$.

Fig. S5 should be compared to Fig. 3b of the text.

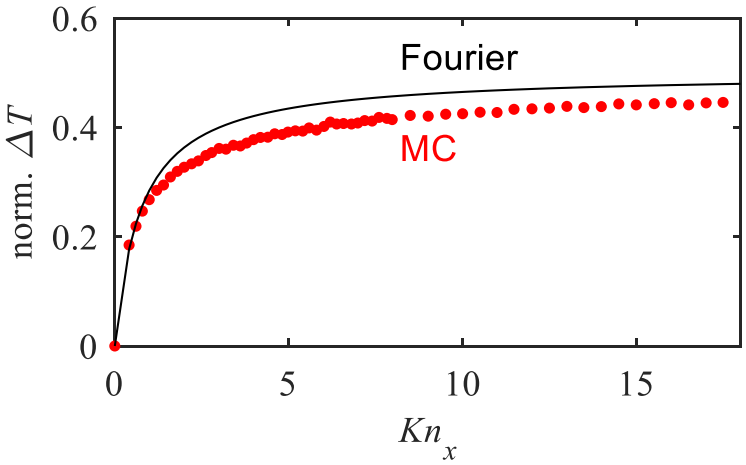

Fig. S5. Normalized temperature jump, $\Delta T\left(x=0\right)/\left(T_L - T_R\right)$ vs. Kn_x for cross-plane thermal transport with no internal heat generation (case 1b in Fig. 1). The Fourier's Law solution (line) is from eqn. (17), and the Monte Carlo solutions of the BTE (symbols) are from [18].

No temperature difference but with internal heat generation

Consider next, the case with no temperature difference between the contacts but with internal heat generation. Figure S6 plots the normalized temperature, $\left(T\left(x\right)-T_b\right)/\left(T_b - T_0\right)$ vs. normalized distance, x/L_x for three different Knudson numbers and compares Fourier's Law to Monte Carlo simulations. For $Kn_x = 0.01$ and $Kn_x = 0.1$ the agreement is excellent while for $Kn_x = 0.5$, the Fourier's Law solution is somewhat below the Monte Carlo solution. As $Kn_x \to \infty$, $\left(T\left(x\right)-T_b\right)/\left(T_b - T_0\right) \to 0$.

Figure S6 should be compared to Fig. 5a in the text.

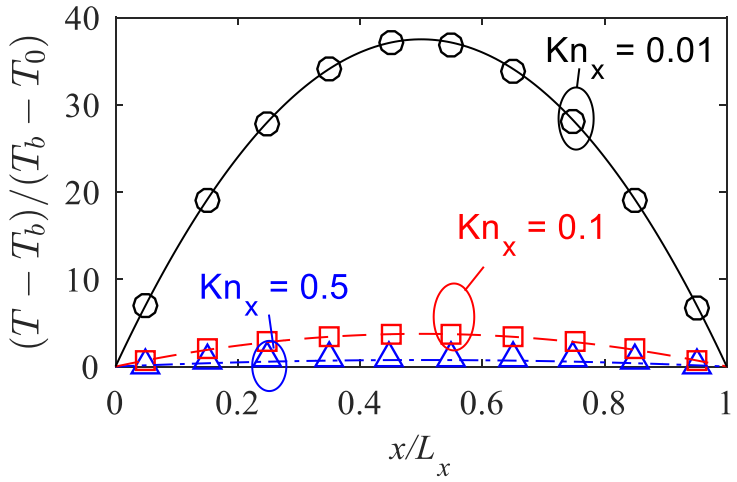

Fig. S6. Nanofilm (cross-plane) with internal heat source. Plot of $\left(T\left(x\right)-T_b\right)/\left(T_b-T_0\right)$ vs. x/L_x for $Kn_x=0.01$, $Kn_x=0.1$, and $Kn_x=0.5$. Lines are Fourier's Law solutions and symbols are the Monte Carlo solutions of [16].

Figure S7 is a plot of the normalized temperature rise, $\delta T/\Delta T$, in the center of the film as given by eqn. (20) vs. Kn_x. Fourier's Law predicts that $\delta T/\Delta T\to\infty$ as $Kn_x\to 0$ and $\delta T/\Delta T\to 0$ as $Kn_x\to\infty$. Good agreement between Fourier's Law and Monte Carlo solutions is observed for small Kn_x. For large Kn_x, $T_{\max}\to T_b$ in both cases, but the Monte Carlo simulations seem to be approaching the correct ballistic limit more slowly than the Fourier's Law solution. We conclude, however, that Fourier's Law provides quite accurate solutions from the ballistic to diffusive limits for this internal heat generation problem.

Figure S7 should be compared to Fig. 5b in the text.

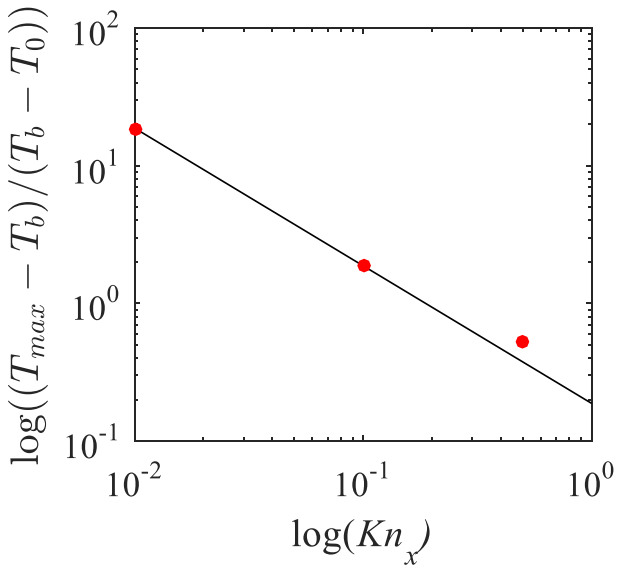

Fig. S7. Normalized temperature rise, $\delta T/|\Delta T|$ vs. Kn_x for cross-plane thermal transport with internal heat generation (case 1b) in Fig. 1). The Fourier's Law solution (line) is from eqn. (20), and the Monte Carlo simulations (symbols) are from [16].

Thin films and nanowires

We turn next to the thin films and nanowires shown in Figs. 1c) – 1f). A proper treatment of these structures requires a two-dimensional solution. Extension of the methods described here to two and three dimensions is needed, but beyond the scope of this paper. Instead, we will examine one-dimensional (1D) solutions to these problems and show that 1D solutions can be quite accurate.

Following Hua and Cao, we examine the apparent thermal conductivity for the structures shown in Figs. 1c) – 1f). Equation (15) gave the apparent thermal conductivity for the case of a temperature difference between contacts with no internal heat generation. In terms of the mean-free-path for backscattering in the bulk, λ, eqn. (15) in the text can be written as

$$\kappa_{app} = \frac{C_v v_x^+ \lambda/2}{1+\lambda/L_x} \ . \tag{S54}$$

In a thin film or nanowire, the mean-free-path is shortened by boundary scattering to

$$\frac{1}{\lambda} \rightarrow \frac{1}{\lambda} + \frac{1}{\beta d} \ , \tag{S55}$$

where β is an empirical parameter and $d = L_y$, the thickness of the film or $d = D$, the diameter of the nanowire. Equation (S55) can be regarded as an empirical fit to more rigorous treatments like that of Fuchs-Sondheimer [27] and McGaughey et al. [28]. Using

(24) in (23) and expressing the result in terms of the Knudson numbers $Kn_x = \Lambda/L_x$ and $Kn_y = \Lambda/d$, we find for the case of a temperature difference (TD),

$$\kappa_{app}\left(TD\right) = \frac{\kappa_{bulk}}{1+\frac{4}{3}\left(Kn_x + Kn_y/\beta\right)}. \tag{S56}$$

Equation (22) gave the apparent thermal conductivity for the case of no temperature difference between contacts with internal heat generation. In terms of the mean-free-path for backscattering in the bulk, λ, eqn. (22) can be written as

$$\kappa_{app} = \frac{C_v v_x^+ \lambda/2}{1+3\lambda/L_x}. \tag{S57}$$

Using eqn. (24) for the mean-free-path in a thin film or nanowire in eqn. (S57) and expressing the result in terms of the Knudson numbers $Kn_x = \Lambda/L_x$ and $Kn_y = \Lambda/d$, we find for the case of internal heat generation (IHG),

$$\kappa_{app}\left(IHG\right) = \frac{\kappa_{bulk}}{1+\frac{4}{3}\left(3Kn_x + Kn_y/\beta\right)}. \tag{S58}$$

Thin film in the diffusive limit $Kn_x << 1$

For a long nanofilm, transport is diffusive in the x-direction, $Kn_x \to 0$, so eqns. (25) and (27) give the apparent thermal conductivities as

$$\kappa_{app}\left(TD\right) = \kappa_{app}\left(IHG\right) = \frac{\kappa_{bulk}}{1+\frac{4}{3\beta_{tf}}Kn_y}. \tag{S59}$$

We can also compute the apparent thermal conductivity from the Fuchs-Sondheimer equation assuming diffusive boundary scattering (specularity parameter, $p = 0$) [27],

$$\kappa_{app}\left(\mathrm{FS}\right) = \kappa_{bulk}\left\{1 - \frac{3Kn_y}{2}\int_1^\infty \left(\frac{1}{t^3}-\frac{1}{t^5}\right)\left(1-\exp\left(-t/Kn_y\right)\right)dt\right\}. \tag{S60}$$

Figure S8 compares the results of various approaches. First, note that in contrast to the Fourier's Law prediction of eqn. (28), the apparent thermal conductivities for the case of a temperature difference is slightly higher than for the case of internal heat generation. The cause for this difference is not clear. Second, note that the Fuchs-Sondheimer equation agrees well with the Monte Carlo simulations for the TD case. Finally, note that the simple Fourier's Law approach with an empirical $\beta_{tf} = 2.9$ agrees well with the Monte Carlo results for the TD case and with the Fuch-Sondheimer results (especially for Kn_y less than about 5). The value, $\beta_{tf} = 2.9$, is between the $3\pi/2$ given by Flik [29] and the 8/3 given by Majumdar [7].

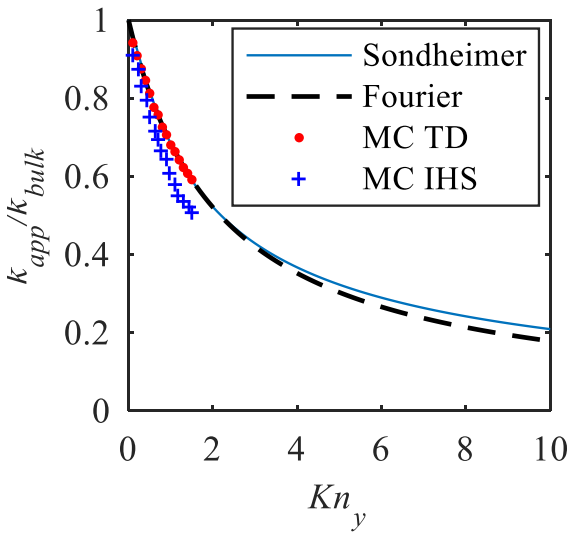

Fig. S8. Apparent thermal conductivity vs. Knudson number, $Kn_y = \Lambda/L_y$ for in plane transport in a diffusive thin film $Kn_x << 1$. Both temperature difference and internal heat generation cases of Fig. 1c) and 1d) are considered. Symbols are Monte Carlo solutions of the BTE [16], the solid line is the Fuch-Sondheimer calculation, eqn. (S56), and the dashed line is the Fourier's Law solution, eqn. (S45), with $\beta_{tf} = 2.9$.

Nanowire from diffusive to quasi-ballistic

For long nanowires, transport is diffusive in the x-direction, $Kn_x \to 0$ so the apparent thermal conductivity is given by eqn. (S55) with $Kn_y = \Lambda/D$, where *D* is the nanowire diameter. For the nanowires with a temperature difference, we can also compute the apparent thermal conductivity from the Fuchs-Sondheimer equation with $p = 0$ [27],

$$\kappa_{app}(TD) = \kappa_{bulk}\left\{1 - \frac{12}{\pi}\int_0^1 dx \int_1^\infty dy \exp\left(-xy/Kn_y\right)\left(1-x^2\right)^{1/2}\left(y^2-1\right)^{1/2} y^{-4}\right\}. \qquad \text{(S61)}$$

Figure S9 compares the three approaches. First, note again that in contrast to the Fourier's Law prediction of eqn. (S59), the apparent thermal conductivities obtained by Monte Carlo simulation for the case of a temperature difference is slightly higher than for the case of internal heat generation. The cause for this difference is not clear. Second, note that the Fuchs-Sondheimer equation agrees well with the Monte Carlo simulations for the TD case. Finally, note that the simple Fourier's Law approach with $\beta_{nw} = 4/3$ agrees well with the Monte Carlo results for the TD case and with the Fuch-Sondheimer results. The value, $\beta_{nw} = 4/3$ is the expected value for a nanowire [27, 28]. Finally, we should mention that the gray model used here (and in [16, 18]) predicts a faster approach to the bulk thermal conductivity with increasing L_y or D than does a non-gray model [28].

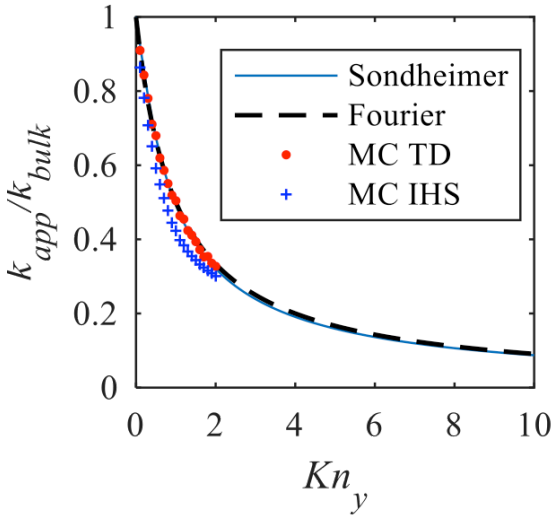

Fig. S9 Diffusive nanowire ($Kn_x \ll 1$). Apparent thermal conductivity vs. Knudson number, $Kn_y = \Lambda/D$ for a diffusive nanowire, $Kn_x \ll 1$. Both temperature difference and internal heat generation cases Fig. 1e) and 1f) are considered. Symbols are Monte Carlo simulation results [16], the solid line is the Fuch-Sondheimer calculation, eqn. (S61), and the dashed line is the Fourier's Law solution, eqn. (S59), with $\beta_{nw} = 4/3$.

Finally, consider the case of an nanowire for $0 < Kn_x < 10$. The apparent thermal conductivities for the TD and IHG cases are given by eqns. (S56) and (S58) for the Fourier's Law solution; in this case, the two apparent thermal conductivities are different. Figure S10 compares the three approaches for $Kn_y = 1$. When Kn_x is just a little greater than zero, the TD and IHG thermal conductivities are predicted by Fourier's Law to be distinctly different. In this case, the agreement with the Monte Carlo solutions of the BTE is much better. (This suggests that one possible explanation for the difference in $\kappa_{app}(\mathrm{TD})$ and $\kappa_{app}(\mathrm{IHG})$ observed in the Monte Carlo simulation results of Fig. S8 might be a numerical artifact due to a length, L_x , that is not long enough to be fully diffusive.)

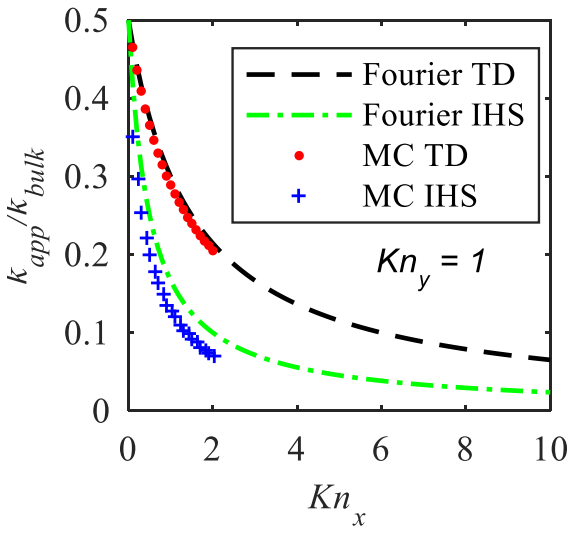

Fig. S10. Apparent thermal conductivities for a nanowire with $Kn_y = 1$ vs. Kn_x. Symbols are Monte Carlo simulation results [16], and the dashed lines are the Fourier's Law solution, eqns. (S52) and (S54) with $\beta_{nw} = 4/3$.

11) Comparison to the solutions of Ordonez-Miranda, et al.

A recent paper by Ordonez-Miranda, et al.:

> Jose Ordonez-Miranda, Rongqui Yang, Sebastien Volz, and J.J. Alvarado-Gil, "Steady-state and modulated heat conduction in layered systems predicted by the analytical solution of the phonon Boltzmann transport equation," *J. Appl. Phys.*, **118**, 075103, 2015.

presented highly-accurate analytical solutions to the phonon BTE under steady-state and small-signal a.c. conditions. In this section, we compare our Fourier's Law solutions to the three steady-state examples considered by Ordonez-Miranda, et al (OM) in Fig. 5 of their paper. The three structures as shown in Fig. S11 below.

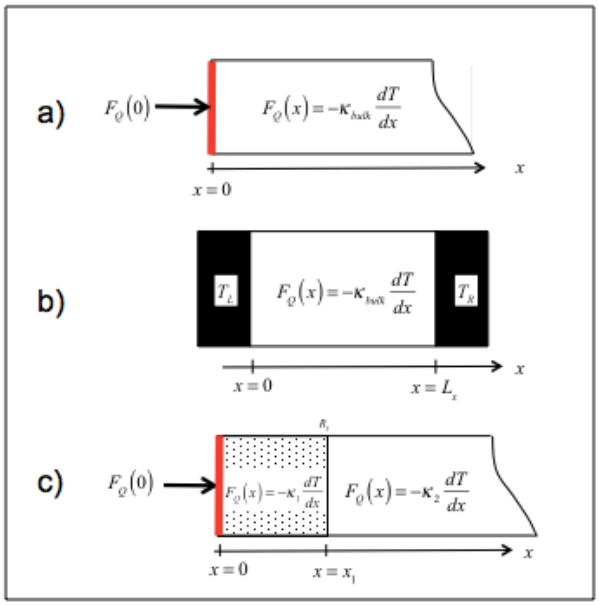

Fig. S11 Three structures considered for steady-state analysis. These are the three structures considered by OM in their Fig. 5.

Consider the semi-infinite example of S11a first and assume that $F_Q(0)$ is a fixed heat generation source at the surface. Fourier's Law gives

$$F_Q(x) = -\kappa_{bulk}\frac{dT}{dx} = F_Q(0), \tag{S62}$$

which can be integrated to determine the temperature:

$$\int_{T(0^+)}^{T(x)} dT = -\int_{0^+}^{x} \frac{F_Q(0)}{\kappa_{bulk}} dx',$$

which can be integrated to find

$$T(x) - T(0^+) = -\frac{F_Q(0)}{\kappa_{bulk}}x. \tag{S63}$$

Now treat the surface as a virtual contact at a temperature, T_0 . Just inside the surface, there is a temperature jump given by

$$\Delta T(0) = T_0 - T(0^+) = F_Q(0)\frac{R_B A}{2}, \tag{S64}$$

where $R_B A/2$ is given by (S29). From (S63) and (S64), we find

$$T(x)=T_0-\frac{F_Q(0)}{C_V v_x^+}\left(1+\frac{C_V v_x^+}{\kappa_{bulk}}x\right). \tag{S65}$$

Using (S19b) for κ_{bulk}, $v_x^+=v/2$, and $\lambda=4\Lambda/3$, we find

$$T_0-T(x)=\frac{3F_Q(0)}{C_V v}\left(\frac{x}{\Lambda}+\frac{2}{3}\right), \tag{S66}$$

which is the Fourier Law solution for the problem of Fig. S11a. The analytical solution of O-M is

$$T_0-T(x)=\frac{3F_Q(0)}{C_V v}\left(\frac{x}{\Lambda}+p(x)\right), \tag{S67}$$

where

$$\frac{1}{\sqrt{3}}=0.58\le p(x)<0.7105. \tag{S68}$$

Comparison of (S66) and (S67) shows the our Fourier's Law solution is the O-M solution with $p(x)=2/3$. The figure below compares the two solutions.

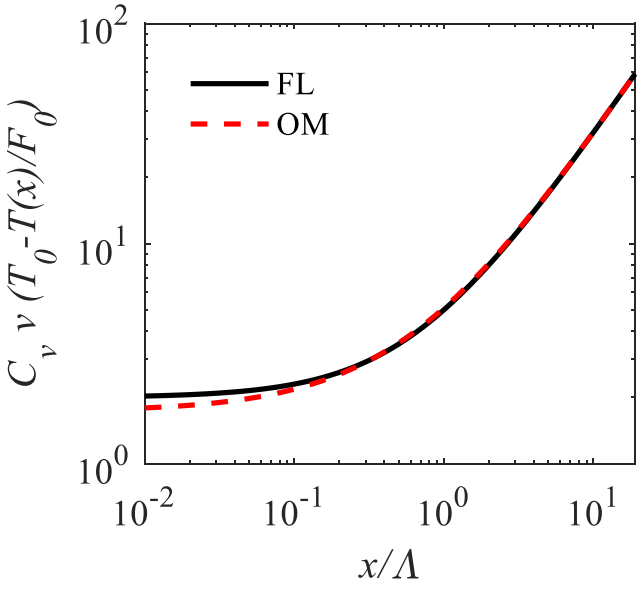

Fig. S12 Comparison of the Fourier's Law and O-M solutions for the problem of Fig. 5a in O-M.

The maximum error in the Fourier's Law solution occurs at $x=0$. From (S66) and (S67) we find

$$\frac{T_0 - T(0)\big|_{\text{FL}}}{T_0 - T(0)\big|_{\text{O-M}}} = \frac{2}{\sqrt{3}} = 1.155, \tag{S69}$$

so the maximum error is less than 16%. Finally, we note that the line in Fig. 5a of O-M labeled "Fourier's Law" should be labeled "Fourier's Law with constant temperature boundary conditions." Our solution, which also assumes Fourier's Law but with appropriate boundary conditions, is much closer to the O-M solution.

Consider next the example in Fig. S11b, which is the case considered in Fig. 1a of the paper. The Fourier's Law solution to this problem is given by eqns. (16) and (17) in the paper:

$$T(x) = (T_L - \Delta T)\left(1 - \frac{x}{L_x}\right) + (T_R + \Delta T)\left(\frac{x}{L_x}\right) \tag{S70a}$$

$$\Delta T = \frac{1}{2}\left(\frac{T_L - T_R}{1 + 3/(4Kn_x)}\right) = \left(\frac{T_L - T_R}{2 + 3L_x/(2\Lambda)}\right). \tag{S70b}$$

Next, we normalize the temperature to that it goes between 0 and 1:

$$U(x) = \frac{T(x) - T_R}{T_L - T_R} = \frac{(T_L - \Delta T)(1 - x/L_x) + (T_R + \Delta T)(x/L_x) - T_R}{T_L - T_R}. \tag{S71}$$

Equation (S67) can be simplified to

$$U(x) = 1 - \left(1 - 2\frac{\Delta T}{T_L - T_R}\right)\frac{x}{L_x} - \frac{\Delta T}{T_L - T_R}. \tag{S72}$$

Equation (17) relates the temperature jump to the Knudsen number/mean-free-path as

$$\frac{\Delta T}{T_L - T_R} = \frac{1}{2 + 3L_x/(2\Lambda)}. \tag{S73}$$

Using (S73) in (S72), we find the Fourier's Law solution to the problem of Fig. S11b as

$$U(x) = 1 - \frac{x/\Lambda + 2/3}{L_x/\Lambda + 4/3}. \tag{S74}$$

The analytical solution of O-M is

$$U_1(x)=\frac{T(x)-T_R}{T_L-T_R}=1-\frac{1}{(L_x/\Lambda)+2\beta}\left[\frac{x}{\Lambda}+\beta+\gamma\left(p(x/\Lambda)-p(L/\Lambda-x/\Lambda)\right)\right]. \qquad \text{(S75)}$$

Equation (S75) provides highly accurate solutions; they agree with the FVM solutions shown in Fig. 3a to within 2%. To relate the O-M solution to the Fourier's Law solution, assume that $p(x)$ is constant (see Fig. 3 in O-M to see how $p(x)$ varies). With this assumption, (S75) becomes

$$U_1(x)=1-\frac{(x/\Lambda)+\beta}{(L_x/\Lambda)+2\beta}. \qquad \text{(S76)}$$

We conclude that the O-M solution reduces to our FL solution if $p(x)$ is constant and if $\beta(x)=2/3$ (see Fig. 4 in O-M for how $\beta(x)$ varies).

Finally, consider the example in Fig. S11c. As given by (S66), the solution in the first layer is

$$T_0-T(x)=\frac{3F_Q(0)}{C_V\upsilon}\left(\frac{x}{\Lambda}+\frac{2}{3}\right) \qquad 0<x<x_1\,. \qquad \text{(S77)}$$

From (S63), we find the solution in the second layer to be

$$T_2(x)-T_2(x_1^+)=-\frac{F_Q(0)}{\kappa_2}(x-x_1) \qquad x>x_1\,. \qquad \text{(S78)}$$

and we just need to find $T_2(x_1^+)$:

$$T_2(x_1^+)=T_1(x_1^-)+\Delta T=T_1(x_1^-)-F_Q(0)R_I\,. \qquad \text{(S79)}$$

From the above equations, we find

$$T_0-T_2(x)=\frac{3F_Q(0)}{C_{V1}\upsilon_1}\left[\frac{C_{V1}\upsilon_1}{C_{V2}\upsilon_2}\left(\frac{x-x_1}{\Lambda_2}\right)+\left(\frac{x_1}{\Lambda_1}+\frac{2}{3}\right)+\frac{R_IC_{V1}\upsilon_1}{3}\right]. \qquad \text{(S80)}$$

By defining a parameter,

$$\delta_{12}=\frac{C_{V1}\upsilon_1}{C_{V2}\upsilon_2}, \qquad \text{(S81)}$$

and assuming the same interface resistance assumed by O-M,

$$R_I = \frac{2}{C_{V1}\upsilon_1} + \frac{2}{C_{V2}\upsilon_2}, \tag{S82}$$

we find the Fourier's Law solution to this problem to be

$$T_0 - T_2(x) = \frac{3F_Q(0)}{C_{V1}\upsilon_1}\left[\delta_{12}\left(\frac{x-x_1}{\Lambda_2} + \frac{2}{3}\right) + \frac{x_1}{\Lambda_1} + \frac{4}{3}\right]. \tag{S83}$$

The analytical solution of O-M is

$$T_0 - T_2(x) = \frac{3F_Q(0)}{C_{V1}\upsilon_1}\left[\delta_{12}\left(\frac{x-x_1}{\Lambda_2} + p(x)\right) + \frac{x_1}{\Lambda_1} + 2\beta(x)\right]. \tag{S84}$$

The Fourier's Law result, (S83), is equal to the O-M result if $p(x) = \beta(x) = 2/3$. The figure below compares the two solutions.

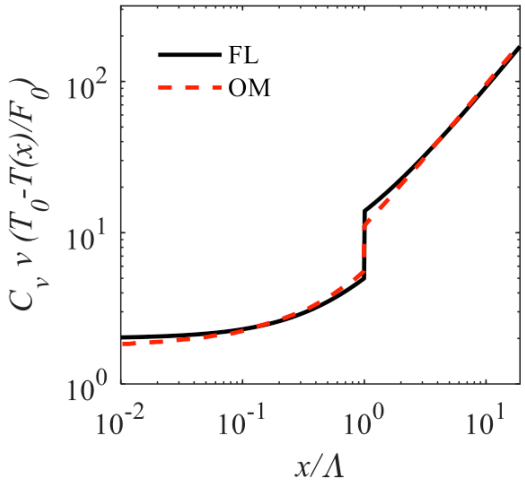

Fig. S13 Comparison of the Fourier's Law and O-M solutions for the problem of Fig. 5c in O-M.

As the above examples show, the Fourier's Law solutions are similar to the highly accurate analytical solutions of O-M et al., but they are not as accurate. Because Fourier's Law is easily applied to a variety of problems for which analytical solutions may not be available, it is useful to know that Fourier's Law can provide approximate solutions at the nanoscale.